novel analytical approaches to characterize particles in biopharmaceuticals

Grabarek, A.D.

Chapter 3

Electrolyte induced formation of submicron particles in heat stressed monoclonal antibody and implications for analytical strategies

Andreas Stelzl[1], Adam D. Grabarek[2,4], Stefan Schneid[3], Wim Jiskoot[2,4], Tim Menzen[2], Gerhard Winter[1]*

[1]*Pharmaceutical Technology and Biopharmaceutics, Ludwig-Maximilians Universität München, Germany*

[2]*Coriolis Pharma Research GmbH, Fraunhoferstr. 18 b, 82152 Martinsried, Germany*

[3]*Bayer AG, Pharmaceuticals, Formulation Development Parenterals, Friedrich-Ebert-Str. 475, 42096 Wuppertal, Germany*

[4]*Leiden Academic Centre for Drug Research, Leiden University, The Netherlands*

Author statements: *Conceptualization:* AS, GW*; Experiment design:* AS, AG, TM, GW*; Methodology:* AS*; Investigation:* AS, AG*; Data analysis:* AS, AG*; Visualization:* AS*; Writing- Original draft:* AS, GW*; Writing- Review & Editing:* AS, AG, SS, WJ, TM, GW*; Resources:* SS, TM, GW

The study presented in this chapter was conducted as part of a collaborative work between Ludwig-Maximilians Universität München and Coriolis Pharma under the lead of Andreas Stelzl. The scope of the study can be considered as the continuation of the research presented in Chapter 2, hence it was included in this thesis. This chapter is in preparation for submission as a manuscript to the *Journal of Pharmaceutical Sciences.*

Abstract

Within this study, the performance and limitations of tunable resistive pulse sensing (TRPS) was evaluated to characterize submicron particles in unstressed and heat stressed monoclonal antibody (mAb) solutions. These were compared with microfluidic resistive pulse sensing (MRPS), resonant mass measurement (RMM), and nanoparticle tracking analysis (NTA). For TRPS and MRPS measurements, adjustment of ionic strength was required but seen critical for protein formulations. Influences of sodium chloride concentration and pH on colloidal stability with respect to submicron particle levels were investigated.

Heat stress caused a sharp increase in particle levels between 250-900 nm, observable in all four techniques. Due to reduced colloidal stability, indicated by increased attractive forces and reduced aggregation onset temperatures in the presence of sodium chloride, protein aggregation was observed in heat stressed mAb only after the addition of sodium chloride. Achieving adequate ionic strength by replacing sodium chloride with other electrolytes similarly resulted in reduced colloidal stability and protein aggregation. It is recommended that protein samples prone for aggregation in the presence of high ionic strength should not be analyzed by RPS measurements after the addition of electrolytes. However, protein samples containing already required ionic strength can be analyzed by any of the four techniques.

Introduction

Biopharmaceuticals, such as monoclonal antibodies, can undergo several routes of degradation due to the complexity of the molecules[1,2]. Among other degradation pathways, the formation of protein aggregates can be detrimental for product quality[3]. Submicron aggregates, despite being often overlooked, are an important category of aggregates due to their potential role in protein immunogenicity[4,5]. However, submicron particle analysis in biopharmaceutical products in the size range of 0.1 – 1 µm is increasingly expected by regulatory agencies[6]. Resonant mass measurement (RMM) and nanoparticle tracking analysis (NTA) are two commonly used methods to quantify the particle level in the submicron size range, but both come with certain drawbacks[7]. NTA is able to detect particles between 50 – 1000 nm based on the scattering of light and is therefore biased towards larger particles if heterogeneous particle populations are measured[7]. Depending on the used sensor, RMM is able to detect particles between 100 – 4000 nm based on their mass, which is then converted it into particle size based on the density of the particle and the density of the fluid[7]. Due to differences in particle detection and subsequent differences in particle characterization, the comparison of results obtained by RMM or NTA can be difficult. For example, a difference of 1-2 orders of magnitude in particle concentration was observed for the same sample when analyzed with both techniques[8]. Additionally, a low reproducibility in particle sizing and quantification compared to established micrometer-sized particle analysis techniques is reported[8].

Owing to improvements in micro- and nano-fabrication[9,10], resistive pulse sensing (RPS) was introduced as new technique for submicron particle analysis. Hereby, the detection of particles in solutions relies on the Coulter counter principle (electrical sensing zone), which detects particles based on changes in the electric field between two electrodes upon particle passage through a sensing orifice[11], thereby overcoming technical limitations of RMM and NTA as discussed above. Studies have shown great accuracy of RPS in characterizing concentration and size of polystyrene bead mixtures or exosomal vesicles, giving RPS a potential advantage over other techniques[12,13].

With tunable resistive pulse sensing (TRPS, IZON Ltd., Christchurch, New Zealand) and microfluidic resistive pulse sensing (MRPS, Spectradyne LLC., Torrance, CA, USA) two RPS-based instruments are currently available for submicron particle characterization. TRPS uses a stretchable nanopore and MRPS a microfluidic channel to create a nano-constriction, which separates both electrodes and can therefore be used as sensing zone. Despite their structural differences, both techniques rely on sufficient ionic strength present in the sample solution[11,14] in order to establish a stable electric current between both electrodes. Thus, particles are detected as drop in electrical resistance by crossing the nano-constriction between both electrodes. For samples with low conductivity, it is recommended to add electrolytes during sample preparation by i.e., dilution in phosphate buffered saline (PBS)[14-16] or by spiking-in electrolytes from a stock solution.

Applicability of RPS for different biopharmaceutical samples including protein formulations was previously presented[17]. In the present study, we investigated the comparability of TRPS to other submicron particle measurement techniques, namely RMM, NTA and MRPS, for the analysis of biopharmaceuticals. Therefore, particle concentrations in the size ranges between 250 - 900 nm and 600 – 900 nm present in an unstressed and heat stressed monoclonal antibody (mAb) formulation were evaluated by using the four instruments and the results were compared. Additionally, the effect of adding electrolytes to (un-)stressed protein formulations prior to particle analysis on the formation of sub-micron proteinaceous particles was critically investigated. A guide to choose a suitable submicron particle characterization technique for biopharmaceuticals based on the conductivity of the samples concludes the paper.

Materials and Methods

Materials

Calcium chloride, glacial acetic acid, L-arginine hydrochloride, L-lysine monohydrochloride, L-methionine, polysorbate 80, sodium acetate, sodium chloride (NaCl), sodium sulfate, and sucrose were purchased from Merck KGaA (Darmstadt, Germany). L-histidine, L-histidine monohydrochloride monohydrate and sodium succinate hexahydrate were purchased from

Alfa Aesar (Kandel, Germany). Magnesium chloride hexahydrate, monosodium phosphate dihydrate, and potassium chloride were obtained from Applichem (Darmstadt, Germany). Citric acid was obtained from USBiological Life Sciences (Hamburg, Germany), disodium phosphate dihydrate from Bernd Kraft (Duisburg, Germany), and sodium citrate from Caesar&Lorentz GmbH (Hilden, Germany). In-house highly purified water (conductivity 0.055 µs/cm) was dispensed from an Arium®Pro purification system (Sartorius, Göttingen, Germany). All diluents used in the study were freshly filtered through a 0.02-µm Anotop 25 syringe filter (Anopore membrane, Whatman, Maidstone, UK).

A mAb (Bayer AG, Leverkusen, Germany), belonging to the IgG1 subclass in 10 mM histidine buffer at pH 5.5 with 130 mM glycine, 5% sucrose, 20 mM methionine, and 0.05% polysorbate 80 was used as model protein. The identical formulation not containing the mAb was used as placebo throughout the study. Different formulations of mAb at pH 4.5 and pH 6.5 were prepared via dialysis at room temperature by using a Spectra/Por® 8000 MWCO dialysis tubing (Spectrum laboratories Inc., Rancho Dominguez, USA). A 100-fold excess of the respective histidine/glycine based formulation was used and media exchanges were performed 2 h and 4 h after the start of the dialysis. Dialysis was performed for a total duration of 24 h.

Coating solution and calibration beads (350 nm, polystyrene) for TRPS measurements were purchased from IZON Ltd. (Oxford, UK) and calibration beads for MRPS (496 nm, polystyrene) and RMM (994 nm, polystyrene) were obtained from Fisher Scientific (Ulm, Germany).

Preparation of proteinaceous particles

All mAb solutions were filtered through a 0.22-µm polyethersulfone (PES) syringe filter prior to use. To generate heat stressed samples, the mAb solution was incubated at 50 °C for 72 h (Eppendorf Thermomix, Hamburg, Germany). Prior to analysis, heat stressed and unstressed samples were diluted to 5 mg/mL mAb concentration by using 0.02-µm filtered placebo solution. The diluted samples were subsequently filtered through a 5-µm PES membrane filter in order to remove large aggregates, if any, which may cause blockages

during submicron particle analysis. Furthermore, the samples were aliquoted for particle analysis and individually spiked with 1 M sodium chloride (0.02-µm filtered) stock solution to a target concentration of 50 mM sodium chloride (e.g., 190 µL sample + 10 µL electrolyte) prior to analysis. Analysis on all four submicron particle characterization techniques as well as micrometer-sized particle analysis were performed within a single working day, but particle analysis was performed not later than 2 min after the addition of sodium chloride to each individual aliquot.

Evaluation of electrolytes to increase conductivity in low-ionic-strength samples for RPS

Stock solutions of eight different electrolytes, $CaCl_2$, KCl, $MgCl_2$, NaCl, Na_2SO_4, histidine buffer pH 6.0, citrate buffer pH 6.0, and phosphate buffer pH 6.0 were prepared as spiking solutions. Concentrations were chosen to reach a conductivity of 4.5 mS/cm after 20-fold dilution and the respective values are given in Table 2. Ten microliter electrolyte stock solution or placebo were added to 190 µL 0.22-µm filtered (PES-membrane) mAb at 5 mg/mL. Because of solubility limits of histidine, required at a relatively high concentration due to low conductivity of histidine solutions, the histidine stock solution was prepared at 450 mM and 20 µL were spiked into 40 µL 5 mg/mL mAb, accounting for a 3-fold dilution of histidine solution. Aggregation onset temperatures were analyzed by using a Prometheus NT.48.

Additionally, submicron particles were characterized by using RMM and NTA after spiking 200 µL placebo, 150 mM sodium chloride, or 450 mM histidine to 400 µL unstressed or heat stressed mAb to investigate the aggregation behavior of the heat stressed mAb in the presence of a high histidine concentration instead of sodium chloride.

Table 2: Conductivity and solute concentration at 4.5mS/cm for various excipients.

Substance class	*Electrolyte*	*Measured conductivity at 50 mM*	*Calculated concentration at 4.5 mS/cm*
		[mS/cm]	*[mM]*
Inorganic salt	$CaCl_2$	2.1	109.2
	KCl	6.2	36.1
	$MgCl_2$	2.2	104.2
	$NaCl$	4.5	50.0
	Na_2SO_4	8.5	26.6
Buffer component	*Citrate buffer, pH 6.0*	8.6	26.2
	Histidine buffer, pH 6.0	1.5	150.0
	Phosphate buffer, pH 6.0	2.4	93.4

Tunable resistive pulse sensing (TRPS)

Submicron particles were analyzed by tunable resistive pulse sensing (TRPS) on a qNano Gold system (IZON, Oxford, UK). A nanopore NP300 with an analysis range of 150 - 900 nm was fitted to the qNano Gold system and submicron particle counts were recorded and evaluated in a similar manner as in our previous study (manuscript in preparation). Three technical replicates per sample were measured.

Microfluidic resistive pulse sensing (MRPS)

A nCS1 system equipped with disposable TS-900 (125 – 900 nm) polydimethylsiloxane cartridges (Spectradyne, Torrance, CA, USA) was used for MRPS measurements. Phosphate buffered saline at pH 7.4 containing 1% polysorbate 20 was used as running buffer to generate an appropriate electrical current. For each sample, the loading volume was 3 µL and at least 500 particles were recorded per measurement. Three technical replicates per sample were analyzed. Size calibration with polystyrene beads (496 nm) was performed for each cartridge after a sample measurement to ensure appropriate sizing. False-positive signals were excluded in data analysis (Data Analysis software V2.4.0.202, Spectradyne) by

applying filters based on transit time, signal-to-noise ratio, peak symmetry, and/or diameter, following the manufacturer's recommendation.

Resonant mass measurement (RMM)

An Archimedes system equipped with a Hi-Q Micro sensor (Malvern Instrument, Malvern, UK) was used for RMM. The system was calibrated with polystyrene beads (994 nm) prior to each set of measurements. Between each sample measurement, 2 sneeze operations were performed, and the system was flushed with highly purified water to ensure system cleanliness. The lower limit of detection (LOD) was determined automatically by ParticleLab software version 2.01. Density was set to 1.05 g/cm³ for polystyrene beads and to 1.34 g/cm³ for protein particles. Only negatively buoyant particles and measurements with at least 50 particle counts were used for data evaluation. Three sub-runs were performed per measurement. Three technical replicates were measured of each sample, yielding nine replicates in total.

Nanoparticle tracking analysis (NTA)

A NanoSight (Model LM20, Malvern Instrument, Malvern, UK) was used to obtain NTA data at a wavelength of 405 nm (blue laser). Purging volume of the sample chamber was 0.3 mL. By using a video capture, three sub-runs of 60 s each were performed per measurement immediately after injection at room temperature. Three technical replicates were measured of each sample, yielding nine replicates in total. The camera levels were set to optimal values and 200 valid tracks were defined as lower limit for valid measurements. NanoSight software version 3.2 was used for data evaluation.

Dynamic light scattering (DLS)

Aggregation onset temperature ($T_{agg,onset}$) and diffusion interaction parameter (k_D) measurements were performed by using a DynaPro plate reader III (Wyatt, Santa Barbara, CA, USA) with a sample volume of 20 µL in 384-well plates (Corning Inc., Corning, NY, USA). Prior to analysis, samples were centrifuged at 2000 g for 2 min and sealed with 5 µL silicone oil to prevent evaporation and centrifuged again for 2 min at 2000 g.

k_D was determined in duplicate with 3-10 mg/mL mAb and different sodium chloride concentrations ranging from 0-150 mM. The diffusion coefficient was obtained from 20 acquisitions at 5 s/acquisition with the attenuation level set to Auto at 25 °C. k_D was evaluated by using Dynamic V7.8.2 software.

$T_{agg,onset}$ of the mAb was determined in formulations containing 5 mg/mL mAb (0.22-µm PES membrane filtered) at pH 4.5, 5.5, or 6.5 after adding 0, 50, and 150 mM sodium chloride. Samples were equilibrated at 25 °C and temperature was increased linearly to 85 °C at a rate of 0.1 °C/min. DLS was measured and each data point was recorded with 3 acquisitions of 3 s per acquisition with the attenuation level set to Auto. $T_{agg,onset}$ was determined in Dynamics V7.8.2 software.

Temperature of aggregation

A Prometheus® NT.48 (NanoTemper Technologies, Munich, Germany) was used to study thermal unfolding and aggregation of mAb formulations. Standard glass capillaries (NanoTemper) were filled with the respective formulation and placed in the Prometheus NT.48 in duplicates. Temperature was ramped from 20 – 95 °C at 1 °C/min. Protein aggregation was detected by measuring the back-reflection intensity of a light beam passing twice through the capillary[18]. The aggregation onset temperature, $T_{agg,onset}$, was calculated with PR.ThermControl V2.1 software (NanoTemper) from the increase in scattering signal detected with the back-reflection optics.

Micrometer-sized particle (SVP) analysis

mAb samples were analyzed for the presence of micrometer-sized particles (sized within the range of 1 – 80 µm) with a FlowCam 8100 (Fluid Imaging Technologies, Inc., Scarborough, ME, USA). The system was equipped with a 10x magnification and a FOV80 flow-cell (80 µm × 700 µm). A sample volume of 150 µL was used for the analysis and the images were collected with a flow rate of 0.15 mL/min with an auto image frame rate of 28 frames/second. A distance of 3 µm to the nearest neighbor and thresholds of 10 and 13 for light and dark pixels, respectively, were used for particle detection. Particle size was

reported as equivalent spherical diameter (ESD) by using VisualSpreadsheet® 4.7.6 software for data collection and evaluation.

Size exclusion chromatography (SEC)

A Dionex Ultimate 3000 system (Thermo Scientific, Dreieich, Germany) was used for SEC. Ten microgram of mAb were injected on a Waters Acquity UPLC® Protein BEH SEC column, 200Å, 1.7 µm, 4.6 × 150 mm column (Waters Corporation, Milford, MA, USA) and the elution of the protein was detected at 280 nm with a VWD-3400RS UV detector (Thermo Fisher, Dreieich, Germany). The running buffer consisted of 50 mM sodium phosphate (pH 6.5) with 300 mM sodium chloride at a flowrate of 0.3 mL/min. The chromatograms were integrated with Chromeleon V7.2 (Thermo Fisher) and the relative area of the high-molecular-weight species (i.e., small soluble aggregates) was calculated in percentage.

Viscosity

The viscosity of the prepared samples was measured by a mVROC viscometer (Rheosense Inc., San Ramon, CA, USA) using a RA05-100-087 flow cell with a 50 µm flow channel at 20 °C. Prepared samples were filled into a 250-µL Hamilton syringe, without introducing any air bubbles. All measurements were performed at a flow rate of 250 mL/min and a corresponding shear rate of 3160 s^{-1}. Control software V2.6 was used for data recording.

Protein concentration

Protein concentration was determined on a NanoDrop One (Thermo Scientific) by measuring the absorbance at 280 nm with a baseline subtraction at 340 nm. Protein concentrations were calculated using a mass extinction coefficient of 13.7 at 280 nm for a 1% w/v IgG solution.

Conductivity measurements

Electric conductivity of samples was measured in triplicate at 20 °C by using an Inolab Cond Level 2 P conductivity meter equipped with a TetraCon 325 electrode (WTW, Weilheim, Germany) calibrated with a 100 µS/cm standard.

Results and discussion

Comparison of submicron particle characterization techniques

Submicron particle concentrations in placebo, unstressed and heat stressed protein (5 mg/mL mAb) samples were determined by using four different submicron particle characterization techniques. Particle size distributions were compared as obtained and particle concentrations were compared in the ranges between 250 - 900 nm and 600 - 900 nm.

Particle size distribution

The average particle size distributions of three replicates measured for unstressed and heat stressed mAb with any of the four particle characterization methods are shown in Figure 1. A bin size of 10 nm was applied to the obtained data for all four methods, however, the scale of the y-axis was varied in order to compare the observed particle size distributions due to differences in the observed particle concentration between the four analytical methods as discussed in section 0. Quantitative descriptors of the particle size distributions of unstressed and heat stressed mAb as such as mean diameter, mode of the peak and D10/D50/D90 values, corresponding to the diameters below which 10%, 50% and 90% of the particles are measured, are provided in

Table 3[19,20]. TRPS and MRPS measurements revealed a narrow particle size distribution with the vast majority of particles detected below 400 nm. RMM revealed substantial particle concentrations for particles above 600 nm, which were hardly detected with both RPS techniques. However, the high LOD values determined with heat stressed mAb samples resulted in no detected particles below 500 nm. Placebo and unstressed samples resulted in much lower LOD values in RMM measurements compared to heat stressed mAb formulations, however no particles below 250 nm were detected. NTA showed the broadest size distribution ranging from 150 nm to 900 nm with a large fraction of particles being larger than 400 nm.

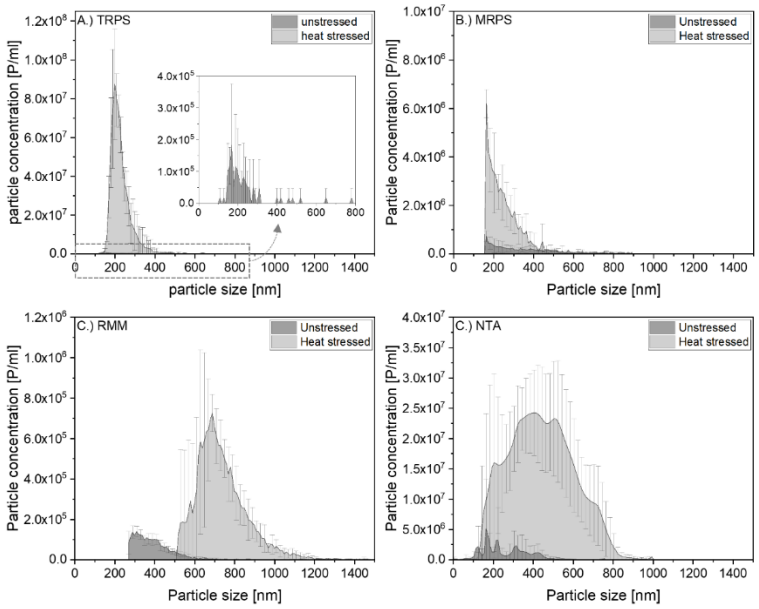

Figure 1: Particle size distribution of unstressed and heat stressed mAb formulation determined by A.) TRPS, B.) MRPS, C.) RMM, and D.) NTA. Error bars represent mean ± standard deviation (10 nm bin size) of three technical replicates. Samples were analyzed at 5 mg/mL protein concentration, except for RMM analysis of heat stressed mAb (2.5 mg/mL). All samples were spiked with 50 mM sodium chloride prior to particle analysis.

Table 3: Quantitative descriptors of the particle size distributions of unstressed and heat stressed mAb formulation

		Mean diameter [nm]	**Mode** [nm]	**D10*** [nm]	**D50*** [nm]	**D90*** [nm]
Unstressed	TRPS	232	170	150	195	305
	MRPS	358	165	170	305	625
	RMM	369	290	280	350	470
	NTA	258	165	125	225	410
Heat stressed	TRPS	226	200	175	210	280
	MRPS	250	165	165	225	355
	RMM	733	690	590	710	890
	NTA	441	405	225	430	655

*** D10/D50/D90 correspond to the diameters below which 10%, 50% and 90% of the particles are measured**

Particle concentration in the size ranges 250-900 nm and 600-900 nm

The comparison of particle concentrations for placebo, unstressed and heat stressed mAb formulations obtained by the four different techniques is shown in Figure 2 and Figure S1 (supplementary data). In contrast to Hubert et al.[8], particle concentrations were compared in the limited size ranges from 250 nm to 900 nm and 600 nm to 900 nm, to eliminate biases due to different size ranges inherent to the four methods.

All submicron particle characterization techniques detected an increase in particle concentration after three days of heat stress at 50 °C compared to an unstressed protein control (Figure 2 and Supplementary figure S1). A narrow standard deviation of the analyzed replicates indicated a high precision in concentration determination for all four methods. However, absolute particle concentrations differed between the four measurement techniques. Between 250 – 900 nm, MRPS and TRPS detected particle concentrations of $6.5x10^7$ and $2.0x10^8$ particles/mL in heat stressed mAb samples, respectively, whereas no increase in particle concentration was observed in the size range from 600 – 900 nm. In the 250 – 900 nm size range, particle concentration in heat stressed mAb samples was highest in NTA with $9.6x10^8$ particles/mL and lowest in RMM with $2x10^7$ particles/mL. Both methods also detected a significant increase in particle levels in the size range above 600 nm. Overall, particle levels in heat stressed mAb samples detected by NTA were found to be 7.5- to 30-fold higher than particle levels obtained by RMM in the size ranges from 600 nm to 900 nm and 250 nm to 900 nm, respectively. An increase in particle concentration after heat stress in the 250 – 900 nm size range was observed with a minimum of 3-fold in RMM and up to 35-fold in NTA compared to the unstressed mAb samples. In the size range from 600-900 nm, the difference in particle concentration between unstressed and heat stressed mAb was up to three orders of magnitude.

In general, placebo formulations showed the lowest particle concentrations with up to two orders of magnitude lower concentrations measured than in unstressed protein samples. However, especially for clean samples, particle concentrations and particle size distributions relied on less than 50 detected particles for TRPS and RMM. In placebo samples, for example, less than 10 particles were typically detected within a measurement time of

10 min (TRPS) or in a measurement volume of 150 nL (RMM). After heat stress, all results derived from any of the four instruments relied on at least 500 particles per measurement for evaluation of the particle size distribution and the particle concentration.

The substantial differences in the submicron particle levels in stressed formulations detected by the four techniques was not only influenced by a high LOD value in RMM, as described in the previous section, but also by differences in particle detection between the methods[7]. For example, differences in particle concentration between RMM and NTA have been reported previously for various protein formulations with higher particle concentrations being detected in NTA, whereas RMM and MRPS showed only minor differences in particle concentration in stressed BSA samples[8,17,22,24]. Comparability of the particle concentrations obtained by either of the four methods is restricted by the underlying physical parameters that are used to detect particles in solution. Additionally, an adjustment of the ionic strength was required for TRPS and MRPS measurements, but is seen critical for protein formulations. Influences of sodium chloride concentration and pH on colloidal stability with respect to submicron particle formation was therefore investigated.

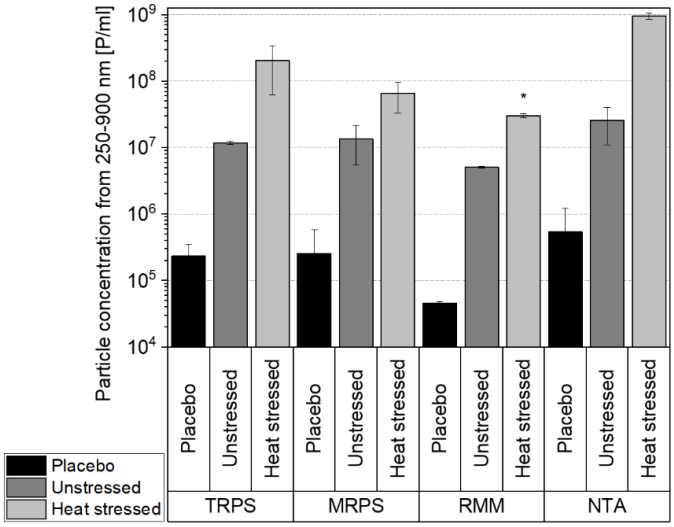

*Figure 2: Comparison of particle concentrations in the size range from 250-900 nm measured by four submicron particle characterization techniques for placebo, unstressed and heat stressed mAb formulations. Error bars represent mean ± standard deviation of three technical replicates. * Particle concentration was analyzed at 5 mg/mL protein concentration, except for RMM analysis of heat stressed mAb (2-fold diluted sample was analyzed and particle concentration was corrected for dilution afterwards). All samples were spiked with 50 mM sodium chloride prior to particle analysis.*

Dimers, oligomers and micrometer-sized particles

Particle concentrations in a size range above 1 µm were measured with flow imaging microscopy (Supplementary figure S2). Total particle concentrations in placebo and unstressed mAb samples were below 400 particles/mL above 1 µm. A slight increase to 1200 particles/mL was detected after heat stress.

The content of dimers and oligomers (Supplementary figure S2) as well as viscosity (1.4 ± 0.1 mPas) and protein concentration remained unchanged after heat stress.

Sodium chloride-induced aggregation through spiking to heat stressed mAb

The addition of electrolytes can be necessary to provide sufficient ionic strength for both RPS methods to achieve reliable results[17]. To investigate the effect of adding electrolytes,

RMM and NTA were used to analyze the submicron particle concentration in samples with and without electrolyte addition (Figure3). Increasing ionic strength in unstressed mAb samples resulted in no change in submicron particle concentration in NTA measurements and only in a minor increase in particle concentration in RMM measurements. The addition of sodium chloride to heat stressed samples led to immediate particle formation, resulting in a 25-fold increase in particle concentration in RMM measurements for the entire size range measured. In NTA, the particle concentration in heat stressed mAb without sodium chloride spiking was already close to the upper limit of the measurement range of 10^{10} particles/mL[23], but an increase was still observed upon addition of sodium chloride prior to particle analysis.

In order to understand the aggregation phenomenon in heat stressed mAb solutions after adding sodium chloride, protein interactions and thermal stability of the mAb was investigated. At pH 5.5, the mAb is positively charged (isoelectric point (IEP): 8.2) and thus net repulsive electrostatic forces inhibit attractive interactions and thus stabilize the molecules from forming aggregates. Shielding positive charges by ions has been found as a cause of protein aggregation[24]. We found that the k_D was only slightly negative with -7.5 mL/g at pH 5.5 (without sodium chloride), indicating weak attractive forces between antibody molecules (Figure 4)[25]. However, k_D rapidly dropped to more negative values upon addition of small amounts of sodium chloride. At 50 mM sodium chloride, the concentration needed for RPS measurements, k_D was reduced to -29 mL/g. The decrease in k_D in the presence of sodium chloride indicates an increase in net attractive protein interactions, probably because of a decrease in repulsive electrostatic interactions. The increase in attractive protein interactions is a likely cause for aggregation of the heat stressed mAb as discussed in the previous sections.

To further assess aggregation behavior of the mAb, $T_{agg,onset}$ was determined for antibody formulations at different pH values (pH 4.5, 5.5, and 6.5) and at different sodium chloride levels (0, 50, and 150 mM sodium chloride) by temperature-ramped DLS and Prometheus measurements. An increase in pH towards the IEP of the protein reduces the net-charge of the protein whereas decreasing pH results in higher net-charge[26]. Increased net-charge was

reported to show the highest degree of repulsion and the addition of sodium chloride was furthermore found to decrease repulsive forces (via charge shielding) for various antibodies[26]. We therefore hypothesize that at lower pH (i.e., higher net charge and therewith stronger repulsive forces between protein molecules), protein aggregation should occur at higher temperatures or at higher sodium chloride concentrations compared to mAb solutions at higher pH.

Without sodium chloride, aggregation was found only in pH 6.5 samples (Figure 5A), whereas aggregate formation was not observed at pH 4.5 and 5.5. Increasing the ionic strength by adding 50 mM sodium chloride led to aggregation in pH 5.5 and 6.5 samples (Figure 5B) with a $T_{agg,onset}$ reduced from > 95 °C and 76.5 °C to 76.3 °C and 72.6 °C, respectively. At pH 4.5 only a weak scattering signal was detected at 50 mM sodium chloride, suggesting that less aggregation occurred compared to the formulations at higher pH value. At a concentration of 150 mM sodium chloride (Figure 5C), the charge shielding effects of sodium chloride supposedly overpowered electrostatic repulsion between mAb molecules, resulting in aggregation in all samples to a comparable extent. Similar trends were found in $T_{agg,onset}$ determined by using DLS (supplementary data, Figure S3).

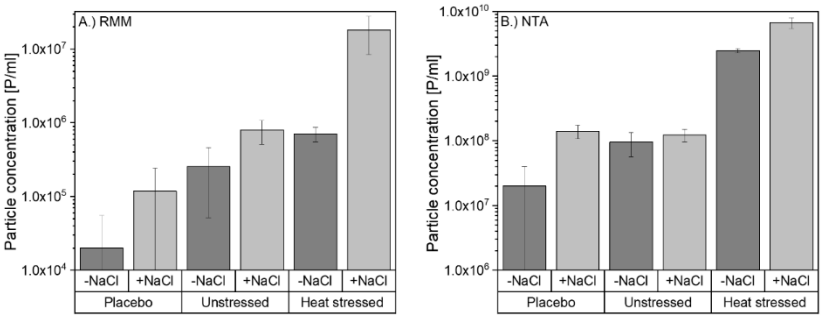

Figure 3: Submicron particle concentration with and without sodium chloride spiking, as determined by A.) RMM and B.) NTA. Mean ± standard deviation of triplicate measurements for the entire size range measured.

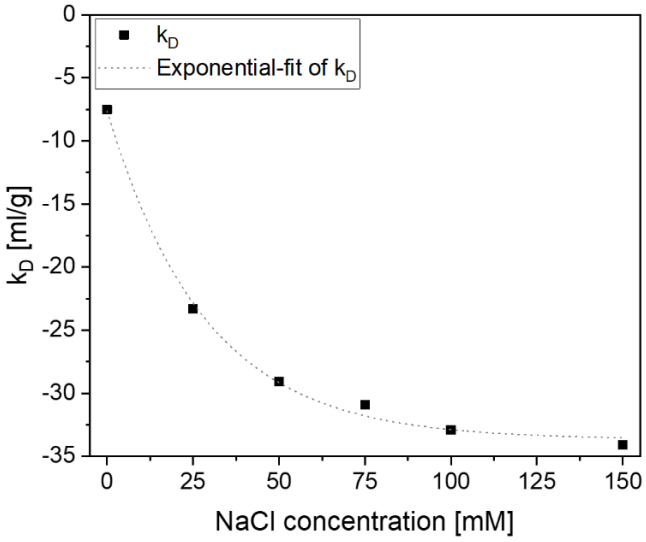

Figure 4: Dependence of kD as a function of sodium chloride concentration in the mAb formulation at pH 5.5.

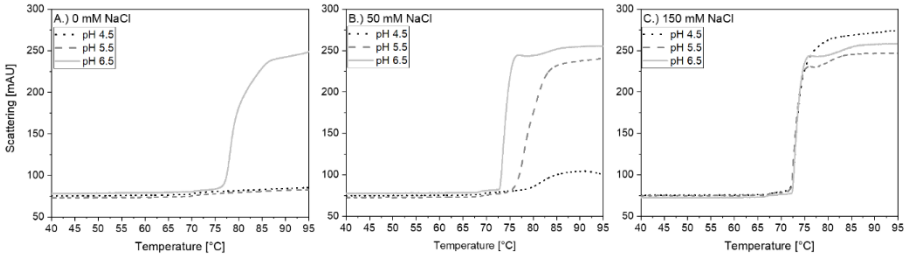

Figure 5: Scattering signal in Prometheus measurements at different formulation pHs and sodium chloride concentrations: A.) 0 mM sodium chloride, B.) 50 mM sodium chloride, C.) 150 mM sodium chloride.

Evaluation of other electrolytes as alternative to sodium chloride

Addition of alternative electrolytes, which provide sufficient conductivity to allow submicron particle analysis by using RPS without inducing so strong mAb aggregation, was evaluated. Tested electrolytes include inorganic salts and buffer components (Table 1).

All tested electrolytes showed a similar scattering signal compared to sodium chloride with aggregation onset temperatures ranging from 69.9 °C to 74.4 °C (Figure 6). None of the tested electrolytes revealed a significantly different result compared to sodium chloride.

The spiking of histidine, replacing sodium chloride as spiking solution, was investigated since histidine was already present in the formulation at a lower concentration. RMM and NTA measurements were conducted after spiking placebo, 150 mM sodium chloride, or 450 mM histidine into unstressed or heat stressed mAb formulation. Thereby, the conductivity was either unchanged when placebo was added to the sample or the conductivity was increased to a level suitable for both RPS techniques with an addition of 150 mM histidine or 50 mM sodium chloride to the sample after spiking with either of the electrolytes. Both, RMM and NTA, showed an increase in submicron particle concentration in heat stressed mAb samples in the presence of additional histidine (Figure 7). The behavior was similar to sodium chloride spiking: Particle formation was not observed when the conductivity was not changed by spiking in placebo solution, and particle formation was not observed in unstressed mAb upon addition of placebo, sodium chloride or histidine.

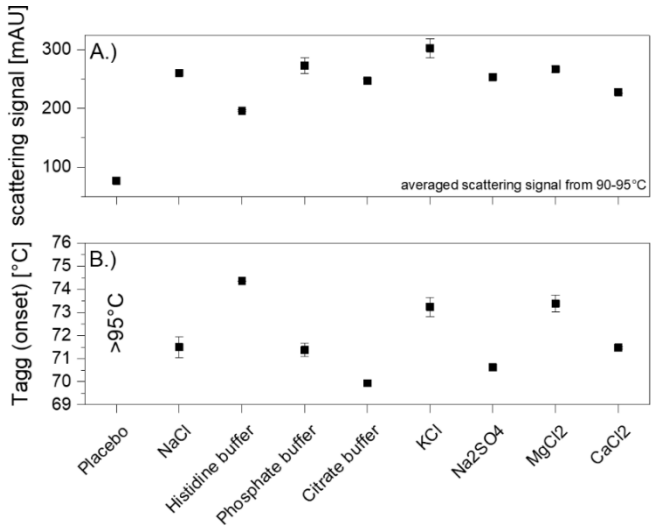

Figure 6: Aggregation of the mAb at pH 5.5 with different electrolytes at a conductivity of 4.5 mS/cm or placebo as control in Prometheus measurements. A.) Averaged light scattering signal in the temperature range from 90 °C to 95 °C, B.) Aggregation onset temperature.

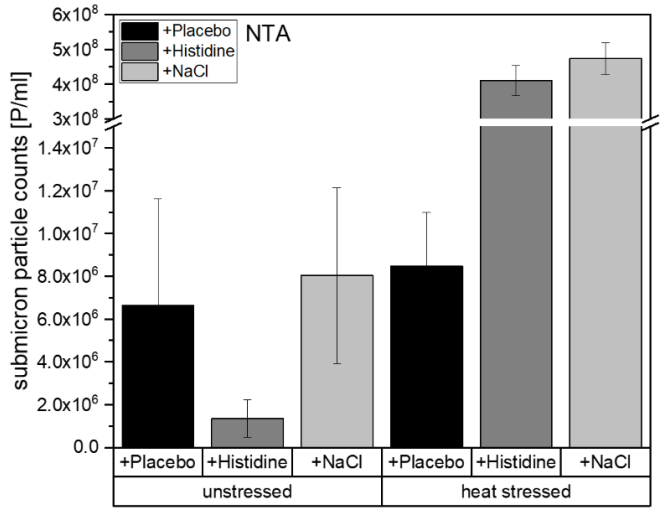

Figure 7: Submicron particle concentrations from NTA with placebo, histidine, or sodium chloride spiking to unstressed or heat stressed mAb. Mean ± standard deviation of triplicate measurements.

Conclusion and selection guide for submicron particle characterization methods

Four submicron particle characterization techniques were compared with regards to their capabilities of quantifying and characterizing submicron particles in proteinaceous samples. Based on previously published work[17], an electrical conductivity exceeding 3 mS/cm or 4.5 mS/cm is required for MRPS or TRPS measurements, respectively, and by spiking-in electrolytes from a stock solution, suitable measurement conditions could be achieved for samples of low ionic strength. A sharp increase in SMPs after three days of heat stress at 50°C compared to unstressed mAb samples was observed by each submicron particle characterization technique and replicates yielded in a narrow standard deviation indicating a high precision in concentration determination for all four methods. Predominantly smaller particles below 400 nm were detected by both RPS techniques, whereas a larger fraction of particles above 500 nm were detected in

RMM and NTA. A pronounced increase in submicron particle levels up to $2x10^7$ to $1x10^9$ particles per milliliter in the size range from 250 – 900 nm was observed after heat stress, depending on the characterization technique. However, only a minor increase micrometer-sized particles and unchanged dimer and oligomer content were observed. SMP quantification during formulation development is therefore an important parameter to assess aggregation behavior of protein formulations without eventually waiting until aggregates have grown larger.

However, as a conductivity level of larger than 4.5 mS/cm is required for both RPS techniques, electrolyte addition was needed to meet this requirement. The addition of sodium chloride caused protein aggregation in heat stressed mAb samples due to reduced colloidal stability indicated by increased protein-protein interactions and decreased aggregation onset temperatures. The formation of submicron particles in heat stressed mAb samples was observed in RMM and NTA analysis after ionic strength adjustment compared to samples without addition of sodium chloride. The use of other inorganic salt or buffer components, such as histidine, for increasing ionic strength resulted in similar $T_{agg,\ onset}$ temperatures and submicron particle formation after spiking to heat stressed mAb samples. Therefore, the addition of electrolytes in order to increase conductivity of the sample for RPS measurement is not recommended.

Since RPS methods require a certain conductivity for particle detection, we recommend to first determine the conductivity of the sample and in case this complies with the mandatory requirements for RPS analysis, any of the four methods is suitable for submicron particle analysis[17]. If the requirements are not met, only RMM and NTA can be recommended for the quantification of submicron particles since the measurement principle is independent of the ionic strength, giving those two methods an advantage over RPS methods.

References:

1. Le Basle, Y., et al., Physicochemical Stability of Monoclonal Antibodies: A Review. J Pharm Sci, 2020. 109(1): p. 169-190.

2. Mahler, H.C., et al., Protein aggregation: pathways, induction factors and analysis. J Pharm Sci, 2009. 98(9): p. 2909-34.

3. Roberts, C.J., Protein aggregation and its impact on product quality. Curr Opin Biotechnol, 2014. 30: p. 211-7.

4. Kijanka, G., et al., Submicron Size Particles of a Murine Monoclonal Antibody Are More Immunogenic Than Soluble Oligomers or Micron Size Particles Upon Subcutaneous Administration in Mice. J Pharm Sci, 2018. 107(11): p. 2847-2859.

5. Moussa, E.M., et al., Immunogenicity of Therapeutic Protein Aggregates. J Pharm Sci, 2016. 105(2): p. 417-430.

6. U.S. Department of health and human services FDA (Center for Drug Evaluation and Research and Center for Biologics Evaluation and Research), Guidance for Industry: Immunogenicity Assessment for Therapeutic Protein Products. 2014.

7. Hawe, A., et al., Subvisible and Visible Particle Analysis in Biopharmaceutical Research and Development, in Biophysical Characterization of Proteins in Developing Biopharmaceuticals. 2015. p. 261-286.

8. Hubert, M., et al., A Multicompany Assessment of Submicron Particle Levels by NTA and RMM in a Wide Range of Late-phase Clinical and Commercial Biotechnology-Derived Protein Products. J Pharm Sci, 2019.

9. Song, Y., J. Zhang, and D. Li, Microfluidic and Nanofluidic Resistive Pulse Sensing: A Review. Micromachines (Basel), 2017. 8(7).

10. Kozak, D., et al., Advances in Resistive Pulse Sensors: Devices bridging the void between molecular and microscopic detection. Nano Today, 2011. 6(5): p. 531-545.

11. Rhyner, M.N., The Coulter principle for analysis of subvisible particles in protein formulations. AAPS J, 2011. 13(1): p. 54-8.

12. Anderson, W., et al., A comparative study of submicron particle sizing platforms: accuracy, precision and resolution analysis of polydisperse particle size distributions. J Colloid Interface Sci, 2013. 405: p. 322-30.

13. van der Pol, E., et al., Particle size distribution of exosomes and microvesicles determined by transmission electron microscopy, flow cytometry, nanoparticle tracking analysis, and resistive pulse sensing. J Thromb Haemost, 2014. 12(7): p. 1182-92.

14. Anderson, W., et al., Observations of Tunable Resistive Pulse Sensing for Exosome Analysis: Improving System Sensitivity and Stability. Langmuir, 2015. 31(23): p. 6577-87.

15. Vogel, R., et al., A standardized method to determine the concentration of extracellular vesicles using tunable resistive pulse sensing. J Extracell Vesicles, 2016. 5: p. 31242.

16. Maas, S.L., et al., Possibilities and limitations of current technologies for quantification of biological extracellular vesicles and synthetic mimics. J Control Release, 2015. 200: p. 87-96.

17. Grabarek, A.D., et al., Critical Evaluation of Microfluidic Resistive Pulse Sensing for Quantification and Sizing of Nanometer- and Micrometer-Sized Particles in Biopharmaceutical Products. J Pharm Sci, 2019. 108(1): p. 563-573.

18. Söltl F., et al., Analysis of formulation-dependent colloidal and conformational stability of monoclonal antibodies. 2016.

19. Allen, T., Particle Size Measurement, Volume 1: Powder Sampling and Particle Size Determination. 2003, Elsevier B.V.

20. Matteucci, M.E., et al., Drug Nanoparticles by Antisolvent Precipitation: Mixing Energy versus Surfactant Stabilization. Langmuir, 2006. 22.

21. Barnard, J.G., K. Babcock, and J.F. Carpenter, Characterization and quantitation of aggregates and particles in interferon-beta products: potential links between product quality attributes and immunogenicity. J Pharm Sci, 2013. 102(3): p. 915-28.

22. Yoneda, S., et al., Quantitative Laser Diffraction for Quantification of Protein Aggregates: Comparison With Resonant Mass Measurement, Nanoparticle Tracking Analysis, Flow Imaging, and Light Obscuration. J Pharm Sci, 2019. 108(1): p. 755-762.

23. Hawe, A., et al., Submicrometer, micrometer and visible particle analysis in biopharmaceutical research and development, in Biophysical Characterization of Proteins in Developing Biopharmaceuticals. 2020. p. 285-310.

24. Arosio, P., et al., On the role of salt type and concentration on the stability behavior of a monoclonal antibody solution. Biophys Chem, 2012. 168-169: p. 19-27.

25. Shi, S., et al., Method qualification and application of diffusion interaction parameter and virial coefficient. Int J Biol Macromol, 2013. 62: p. 487-93.

26. Lehermayr, C., et al., Assessment of net charge and protein-protein interactions of different monoclonal antibodies. J Pharm Sci, 2011. 100(7): p. 2551-62.

Supplementary materials

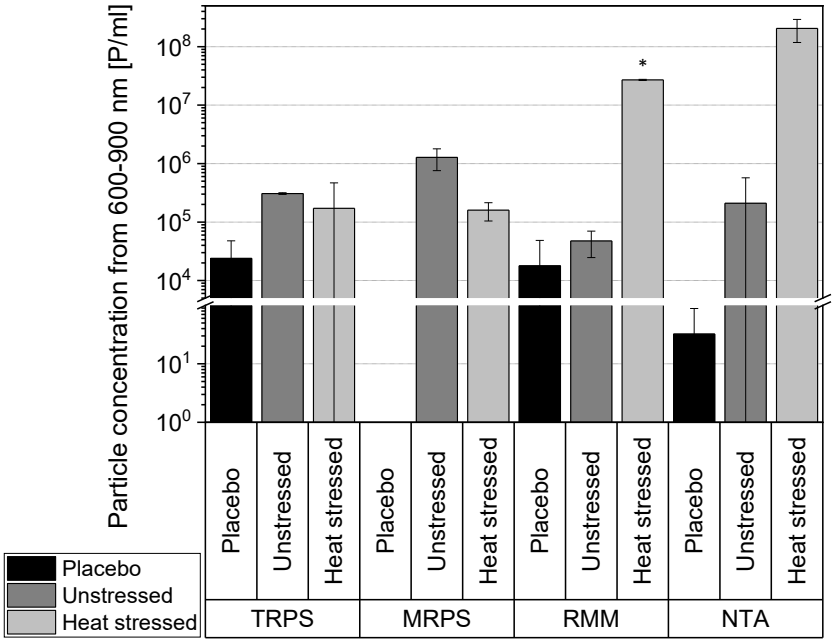

*Supplementary figure S1: Comparison of particle concentrations in the size range from 600-900 nm measured by four different submicron particle characterization techniques for placebo, unstressed and heat stressed mAb formulations. Error bars represent mean ± standard deviation of three technical replicates. * Particle concentration was analyzed at 5 mg/mL protein concentration, except for RMM analysis of heat stressed mAb (2-fold diluted sample was analyzed and particle concentration was corrected for dilution afterwards). All samples were spiked with 50 mM sodium chloride prior to particle analysis.*

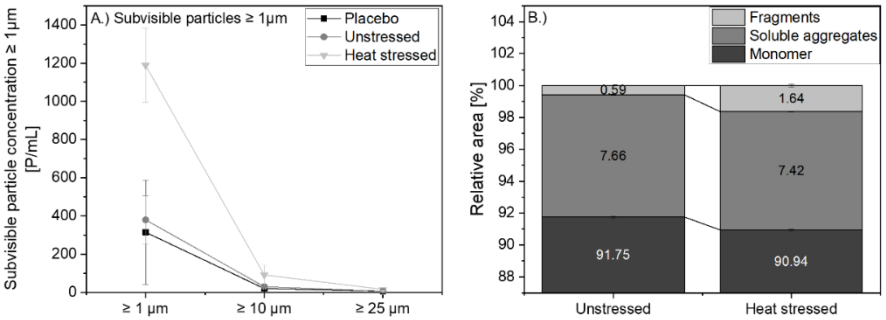

Supplementary figure S2: A.) Subvisible particle concentrations obtained by FlowCam analysis, B.) Relative area of monomers, soluble aggregates, and fragments obtained by size exclusion chromatography. Placebo and unstressed samples were measured at t0, heat stressed samples after 3 days at 50°C.

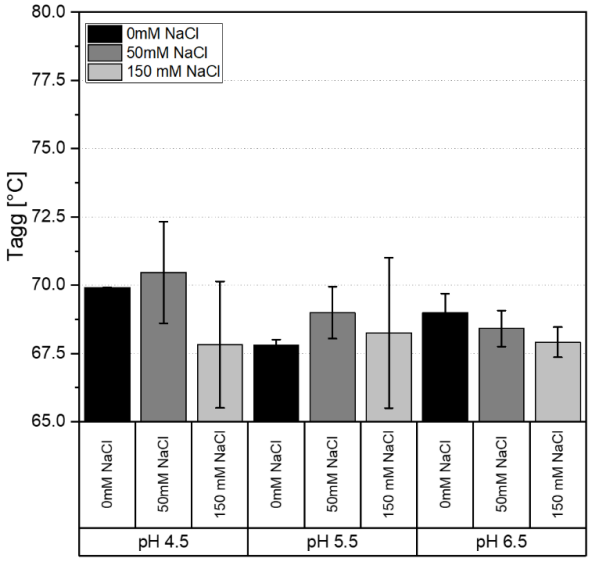

Supplementary figure S3: $T_{agg,\ onset}$ of the mAb at different formulation pHs and sodium chloride concentrations, as determined by using dynamic light scattering.